# CHARACTERIZATION OF VANADIUM SITES ON VANADIUM-CONTAINING MESOPOROUS SILICA CATALYSTS AND THEIR CATALYTIC BEHAVIOUR IN PROPANE ODH

Nikola DRENCHEV, Daniel ŠVADLÁK[1], Michal SETNIČKA,
Pavel ČIČMANEC and Roman BULÁNEK
Department of Physical Chemistry,
The University of Pardubice, CZ–532 10 Pardubice

*Parameters that affect the catalytic behaviour of vanadium-containing mesoporous silicas in oxidative dehydrogenation reaction of propane are mainly aggregation state of surface $VO_x$ species and reducibility of vanadium species. Type and conditions of synthesis have big impact on the nature of vanadium species and, therefore, influence significantly catalytic properties. Two vanadium-containing mesoporous silica catalysts were synthesized by different techniques (including direct synthesis from hydrogel containing vanadium precursor and wet impregnation of SBA-15 mesoporous silica by vanadyl acetylacetonate) and their physico-chemical and catalytic properties were studied and compared. Direct synthesis of vanadosilicate led to catalysts with non-uniform mesoporosity, but exhibiting better spreading of vanadium on the surface resulting in species with*

---

[1] To whom correspondence should be addressed.

*lower degree of polymerization compared to impregnated catalyst. It is reflected in higher iso-conversional selectivity of directly synthesized catalyst towards propene.*

## Introduction

Vanadium catalysts are used in a wide range of heterogeneous catalytic reactions like oxidative dehydrogenation (ODH) of light alkanes, oxidation of several volatile organic compounds, epoxidation reactions and others [1-6]. V-containing mesoporous silicas (e.g., V-SBA-15, V-MCM-41, V-MCM-48, V-MCF, etc.) with uniform pores size and high surface area are interesting catalysts for oxidation reactions, allowing a large concentration of accessible and well defined active centers ($VO_x$), often incorporated into the silica framework [7-11]. Extensive studies have been made on supported vanadium oxides [12-16]. It has been established that the catalytic behaviour is related to parameters such as the oxidation state, coordination number, aggregation state and reducibility of vanadium species. These parameters are influenced not only by the vanadium loading but also by the nature of support and the preparation of catalyst.

It is generally accepted that, at very low vanadia loadings, the surface vanadium oxide species are isolated tetrahedrally coordinated $VO_4$ units. However, increasing vanadia loading on the surface leads to polymerization of surface vanadyls even to bulk vanadium pentoxide. The existence of oligomeric V–O–V species on the $VO_x$ -silica materials with medium vanadium loading is still under debate. The method of the deposition of active vanadium species is a very important parameter which can strongly influence the degree of dispersion and coordination of $VO_x$ units on the surface. The simple wet impregnation method by vanadium salts ($NH_4VO_3$, vanadyl acetylacetonate) is very often used for the deposition of $VO_x$ species. However, this method usually leads to materials with a broad distribution of $VO_x$ species and also formation non-selective bulk-like vanadium oxide with octahedral coordination. The direct hydrothermal synthesis of mesoporous vanadosilicate is an alternative method for incorporation of $VO_x$ species on the silica surface or to the silica wall. Unfortunately, controlling of structural and textural parameters of vanadosilicates prepared by direct synthesis is much more difficult compared to synthesis of pure silica.

Therefore, we report here a comparison of catalytic performance of V-containing high-surface siliceous materials prepared by wet impregnation of SBA-15 silica with well-developed regular mesoporosity and by direct synthesis under conditions mimicking the synthesis of SBA-15 silica in ODH of propane in order to investigate effect of preparation method on the speciation of vanadium complexes and its impact on catalytic behaviour in propane ODH. Prepared catalysts were characterized by XRF for determination of vanadium content, XRD,

SEM and $N_2$-adsorption for study of morphology and texture, and $H_2$-TPR, DR UV-vis and FT-IR spectroscopy for the determination of vanadium complex speciation. All the prepared materials were tested in propane ODH reaction at 540 °C, and obtained catalytic results were correlated with structural and surface characteristics of catalysts.


**Experimental**

Materials

Purely siliceous SBA-15 mesoporous molecular sieve were synthesized as reported earlier [17] using a triblock copolymer, Pluronic P123 ($EO_{20}PO_{70}EO_{20}$, BASF/Aldrich) as a structure directing agent. Tetraethoxysilane (TEOS) was used as a silica precursor yielding a typical synthesis molar ratio $TEOS:HCl:P123:H_2O$ = 1:6.2:0.017:197. The synthesis mixture was vigorously stirred at 35 °C for 5 min and subsequently aged under static conditions for 24 hours at 35 °C and 48 hours at 97 °C. The resulting solid was recovered by filtration, extensively washed out with distilled water and ethanol, and dried at 100 °C overnight. The template was removed by calcination in a stream of air at 540 °C for 8 hours with the heating rate of 1 °C $min^{-1}$. Vanadium oxo-complexes were doped onto silica support (for the sample with 9 wt.% V) by standard wet impregnation procedure by appropriate amount of ethanol/$H_2O$ solution of vanadyl acetylacetonate (Aldrich). The impregnated samples were dried at 120 °C in air overnight and then calcined at 600 °C for 8 hours in the dry air flow.

Directly synthesized vanadosilicate sample was prepared by the following procedure reported by Gao [11]. The Pluronic P123 ($EO_{20}PO_{70}EO_{20}$) of weight of 4.0 g was dissolved in 30.0 g distilled water and stirred for 4 h, whereupon 9.0 g tetraethyl orthosilicate (TEOS) and the appropriate amount of ammonium metavanadate ($NH_4VO_3$) were added directly to the homogeneous solution ($n_{Si}/n_V$ = 10, i.e., ca. 7.4 wt.%). Then a proper quantity of 0.30 M HCl was added to adjust the pH value of reaction mixture to 3.0. The gel was stirred for 24 h and then maintained at 100 °C for another 48 h. The resultant dark-green precipitate was collected, washed thoroughly with distilled water and absolute ethanol for several times and dried at 70 °C for 12 h. The as-prepared product was then calcined in air stream at 550 °C for 6 h with a heating rate of 1 °C $min^{-1}$ to remove the template.

The samples prepared by direct synthesis and impregnation method were labelled as DS and IMP, respectively.

Instrumental Methods

The vanadium content was verified by X-ray fluorescence spectroscopy by ElvaX (Elvatech, Ukraine) equipped with Pd anode. Samples were measured against the model samples (a mechanical mixture of pure $SiO_2$ and $NaVO_3$) granulated to grains 0.25-0.50 mm (the same size as catalysts samples).

X-ray powder diffraction data were recorded on a Bruker D8-Advance diffractometer (Bruker AXE, Germany) in the $2\theta$ range 0.7°-10° on equipped with a graphite monochromator and a position-sensitive detector (Vantec-1) using Cu $K\alpha$ radiation (at 40 kV and 30 mA) in Bragg–Brentano geometry.

The particle morphology of vanadium mesoporous silica was evaluated by scanning electron microscopy using a JEOL JSM-5500LV instrument operated at 20 kV and the high-resolutions transmission electron microscopy (HRTEM) using a JEM-3010 transmission electron microscope with an accelerating voltage of 300 kV and $LaB_6$ cathode. The samples were supported for the experiment on carbon-coated copper grids.

Nitrogen was used as adsorptive and supplied by Messer (Griesheim, Germany — purity 99.999 vol.%). Sorption isotherms of nitrogen at 77 K were determined using an ASAP 2020 instrument. In order to attain a sufficient accuracy in the accumulation of the adsorption data, this instrument is equipped with pressure transducers covering the 133 Pa, 1.33 kPa and 133 kPa ranges. Before each sorption measurement, the sample was degassed to allow a slow removal of the most of pre-adsorbed water at low temperatures. This was done to avoid potential structural damage of the sample due to surface tension effects and hydrothermal alternation. Starting at ambient temperature the sample was degassed at 110 °C (temperature ramp of 0.5 °C min$^{-1}$) until the residual pressure of 1 Pa was attained. After further heating at 110 °C for 1 h, the temperature was increased (temperature ramp of 1 °C min$^{-1}$) until the temperature of 250 °C was achieved. The sample was degassed at this temperature under turbomolecular pump vacuum for 8 h.

Redox behaviour of $VO_x$ surface species was investigated by the temperature programmed reduction by hydrogen ($H_2$-TPR) using the AutoChem 2920 (Micromeritics, USA). 100 mg sample in a quartz U-tube micro-reactor was oxidized in oxygen flow at 450 °C (2 h) prior to the TPR measurement. The reduction was carried out from 100 °C to 900 °C with a temperature gradient of 10 °C min$^{-1}$ in the flow of reducing gas (5 vol.% $H_2$ in Ar). The changes of hydrogen concentration were monitored by the TCD detector.

The UV-vis diffuse reflectance spectra of dehydrated diluted samples were measured using a Cintra 303 spectrometer (GBC Scientific Equipment, Australia) equipped with a Spectralon-coated integrating sphere using a Spectralon coated discs as a standard. The spectra were recorded in the range of the wavelength 190-850 nm. The samples were diluted by the pure silica (Fumed silica, Aldrich) in the

ratio 1:100. All the samples were granulated and sieved to fraction of size 0.25-0.5 mm, dehydrated before the spectra measurement and oxidized in the glass apparatus under static oxygen atmosphere in two steps: 120 °C for 30 min and 450 °C for 60 min and subsequently cooled down to 250 °C and evacuated for 30 min. After the evacuation, the samples were transferred into the quartz optical cuvette 5 mm thick and sealed under vacuum. This procedure guaranteed complete dehydration and defined oxidation state of vanadium for all catalysts. The obtained reflectance spectra were transformed into the dependencies of Kubelka–Munk function $F(R_\infty)$ on the absorption energy $h\nu$ using $F(R_\infty) = (1 - R_\infty)^2/(2R_\infty)$, where $R_\infty$ is the measured diffuse reflectance from a semi-infinite layer [18].

The propane oxidative dehydrogenation reaction (propane ODH) was carried out in a quartz plug-flow fixed-bed reactor at atmospheric pressure in the kinetic region (independently checked) and under steady state conditions of reaction. The activity and selectivity of catalysts were tested at temperature 540 °C in the dependence on contact time (W/F 0.03, 0.06, 0.09 and 0.15 $g_{cat}s^{-1}cm^{-3}$) in order to obtain iso-conversion of propane 13 %. The demanded weight of catalyst (grains 0.25-0.50 mm) was mixed with 2 $cm^3$ of inert SiC. The catalysts were pretreated in the oxygen flow at 540 °C for 2 h before each reaction run. The input feed composition was $C_3H_8/O_2/He$ = 5/2.5/92.5 vol.% with a total flow of 100 $cm^3min^{-1}$ STP. The analysis of reaction mixture composition was made by on-line gas chromatograph Agilent 7890A equipped with TCD and FID detectors. The feed conversion, selectivity to products and productivity were calculated based on mass balance according to Sachtler and Boer [19]. The turn-over-frequency (TOF) values per V atom were calculated according to $TOF = (n^0_{C_3H_8}X_{C_3H_8}M_V)/(m_{cat}w_V)$, where $n^0_{C_3H_8}$ is molar flow of propane (mol $s^{-1}$), $X_{C_3H_8}$ is conversion of propane (%), $M_V$ is atomic weight of vanadium (50.94 g $mol^{-1}$), $m_{cat}$ is weight of catalyst (g), $w_V$ is mass fraction of vanadium in catalysts.

The FT-IR spectra of NO molecules adsorbed on the $VO_x$ species were collected at room temperature using an FT-IR Nicolet 6700 spectrometer (equipped with MCT detector) at a spectral resolution of 2 $cm^{-1}$ and accumulating of 64 scans. Self-supporting wafers (ca. 5-8 mg $cm^{-2}$) were prepared from the sample powder and treated directly into glass IR cell. The cell was connected to a vacuum-adsorption apparatus with residual pressure of $10^{-3}$ mbar. Prior to the adsorption measurements, the samples were activated by heating from ambient temperature to 450 °C for 1 h and then were evacuated at the same temperature for 1 h. A part of vanadium atoms are reduced upon evacuation. Vanadium in 3+ and 4+ oxidation state is oxidizing in the presence of oxygen even at RT. Treatment at 450 °C in atmosphere of pure $O_2$ (40-50 mbar) for 20 min is enough for full oxidation of reduced vanadium atoms. This step was carried out due to be sure that reduction of samples starts from fully oxidized one. The samples were reduced by treatment with hydrogen (400 mbar at 450 °C for 3 h). After reduction, the samples

were evacuated for 1 h at the reduction temperature. Before adsorption, NO was additionally purified by fraction distillation. The spectra obtained through subtraction of the spectrum of the treated sample in vacuum from the spectrum in the presence of the probe molecules are reported here. The spectra are gas phase corrected.

## Results and Discussion

Physicochemical Properties of Samples

The concentration of vanadium determined by XRF method is 9 wt. % and 6.5 wt. % for impregnated and direct synthesis samples, respectively (Table I). It means that almost 90 % of vanadium from synthesis gel was successfully incorporated into silica structure by direct synthesis, and in the case of impregnation method it was 100 %.

Table I    Chemical composition and results of textural characterization of vanadium mesoporous materials

| Sample name | $w_V$[a] wt. % | $S_{BET}$[b] m$^2$ g$^{-1}$ | $V_{ME}$[c] cm$^3$ g$^{-1}$ | $V_{MI}$[d] cm$^3$ g$^{-1}$ | $D_{ME}$[e] nm |
|---|---|---|---|---|---|
| IMP | 9 | 300 | 0.571 | 0.011 | 9.4 |
| DS | 6.5 | 358 | 1.22 | 0 | 8 |
| SBA-15 | 0 | 780 | 0.82 | 0.06 | 10.1 |

[a]Vanadium content determined by XRF method
[b]The BET surface area evaluated using adsorption data
[c]$V_{ME}$ mesopore volume determined by Barret–Joyner–Halenda (BJH) algorithm
[d]$V_{MI}$ micropore volume determined by using the t-plot method
[e]$D_{ME}$ mesopore diameter determined by BJH algorithm

The XRD patterns in the $2\theta$ range 0.7°-10° of samples prepared by impregnation method and direct synthesis are shown in Fig. 1. The samples vary significantly in this patterns, the samples prepared by impregnation method exhibit three well-resolved diffraction lines at 1.02°, 1.73° and 1.98°, which are associated with a long-range order mesostructure typical for two-dimensional hexagonal pore arrangement in p6mm symmetry of the mesoporous SBA-15 and corresponding to Miller indexes (100), (110) and (210) [20-23]. On the other hand, the sample prepared by direct synthesis shows only poorly resolved reflections, which is not purely associated with current ordered pore structure. This is caused by loss of regularity order and by a broad pore size distribution (Fig. 5). Nature and texture of samples was additionally proved by the SEM (Fig. 2) and HR-TEM (Fig. 3). The impregnated sample revealed regular particles with typical morphology  for
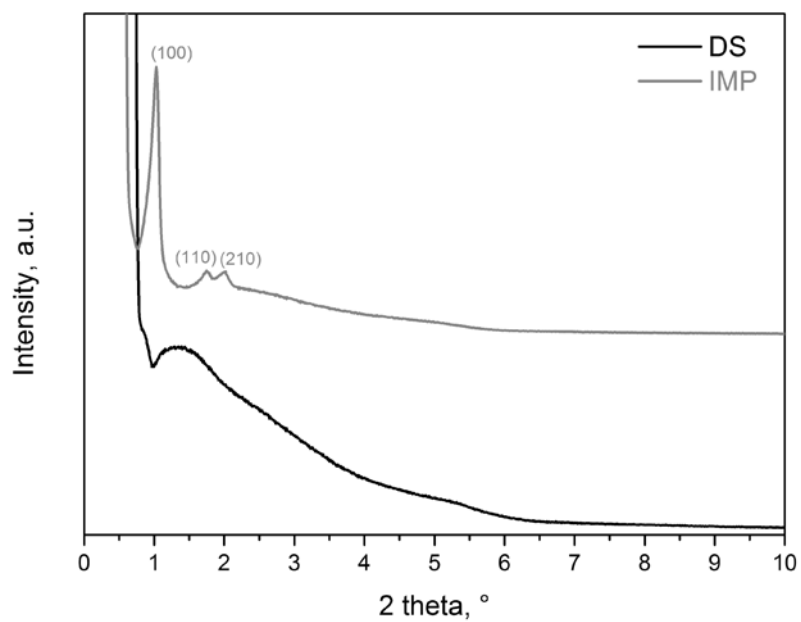
Fig. 1  X-ray diffraction patterns (after calcination) in 2θ range 0.7°-10° for samples prepared by impregnation method (IMP) and direct synthesis (DS)
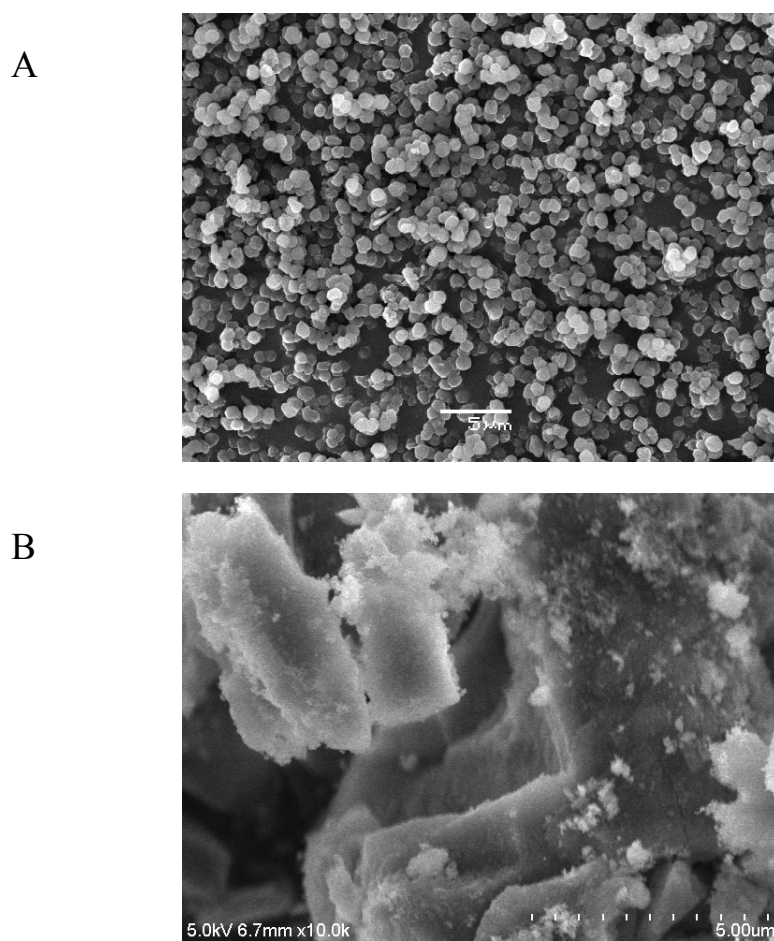


A

B

Fig. 2  Scanning electron micrographs of impregnated (A) and direct synthesis (B) samples

SBA-15 silicas [23,24]. The direct synthesis sample shows larger blocks with small particles on their surface. The TEM images of both prepared samples and parent SBA-15 silica are shown in Fig. 3. The SBA-15 silica (Fig. 3A) shows in detail well-ordered hexagonal array of mesopores system of cylindrical pores. The distance between mesopores from high-dark contrast in the TEM images is estimated ca. 7.6 nm in good agreement with pore size determined from adsorption isotherm. The sample prepared by impregnated method is shown in Fig. 3B. It is evident that the hexagonal arrays of mesopores system are preserved. The dark areas in the figure are the blocked pores (maybe by vanadium oxide clusters or silica plugs formed during the treatment of sample in the solution). The distance between mesopores is estimated ca. 6.9 nm. TEM image of the sample prepared by direct synthesis is depicted in Fig. 3C. This sample exhibits quite different texture. Well-ordered hexagonal array of mesopores is not developed. The material exhibits larger empty space with the size ca. 20-35 nm resembling foam with small areas exhibiting cylindrical pores with a significantly smaller size around 7 nm.

Nitrogen adsorption isotherms for both samples are illustrated in Fig. 4. For impregnated samples, the hysteresis loop (type H1) is very similar to silica support SBA-15 (Fig. 4) or V-SBA-15 catalysts prepared by impregnation method and published in the literature [11,25]. It confirms that modifications of the SBA-15 support by $VO_x$ impregnation did not change significantly the structure of material. On the other hand, the shape of isotherm and hysteresis loop for direct synthesis sample is not similar to SBA-15 silica [21] prepared by impregnation method, but resembles to the isotherms for direct synthesis V-SBA-15 as showed Piumetti *et al.*[9]. For this sample, the isotherm shows type IV with a smoother hysteresis loop exhibiting two poorly resolved condensations. It indicates mesoporosity of the material with nonuniformity of pore size. The mesopore volume ($V_{ME}$) and mesopore size distribution of silica materials were calculated using BJH algorithm calibrated to accurately reproduce the pore diameter and volume (Table I and Fig. 4). The impregnated sample shows the value of mesopore volume 0.571 $cm^3 g^{-1}$ and pore diameter 9.4 nm. These values are smaller in comparison with SBA-15 silica (0.820 $cm^3 g^{-1}$; 10.1 nm) which is the consequence of $VO_x$ species which are anchored on the silica surface and occupy partially the space in the pore . The direct synthesis method leads to the material exhibiting significantly larger volume of mesopores (1.22 $cm^3 g^{-1}$). The pore size distribution in DS sample (see Fig. 5) is wider in comparison with the sample prepared by the impregnation method and exhibits bimodal character. The main peak is centered at 8 nm and secondary wide shoulder covers a range from 10 to 30 nm. We suppose that pores with ca. 8 nm come from partially developed structure of cylindrical pores (as is visible on TEM image), while foam part of material is reflected in a broad distribution peak at larger diameters. Such dual porosity should be a benefit of this material, because larger pores improve mass transport through catalyst and such catalyst can find application in conversion of larger molecules for example higher hydrocarbons,
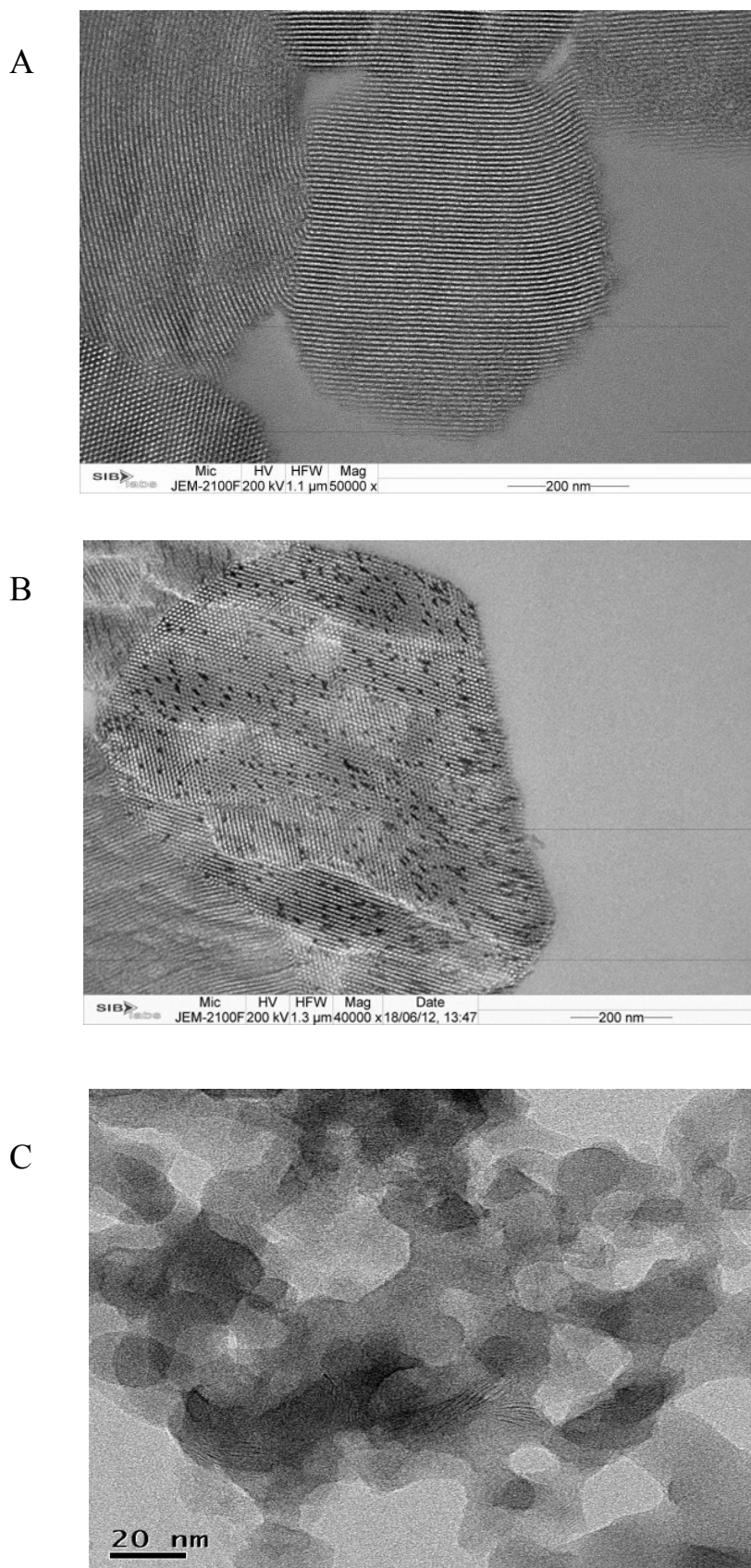
A

B

C

Fig. 3   Transmission electron microscopy images of SBA-15 silica (A), sample prepared
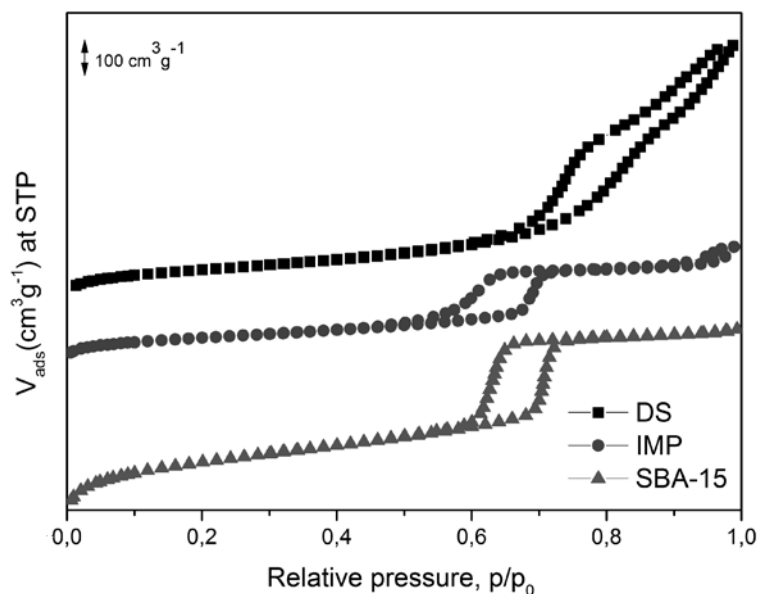by impregnation method (B) and direct synthesis (C)

Fig. 4  $N_2$ adsorption/desorption isotherms of samples prepared by impregnation method (IMP), direct synthesis (DS) and pure silica SBA-15
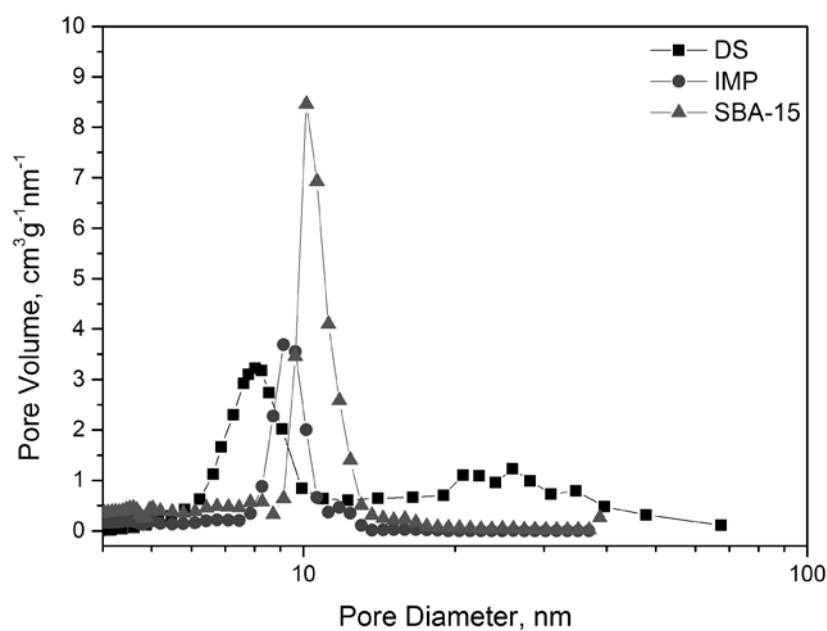


Fig. 5  Pore size distribution for samples prepared by impregnation method (IMP), direct synthesis (DS) and pure silica SBA-15

higher alcohols and aromatic molecules [7,26]. The BET surface areas evaluated using adsorption data in a relative pressure range from 0.05 to 0.25 are summarized in Table I. The total surface areas ($S_{BET}$) are 300 m$^2$ g$^{-1}$ and 358 m$^2$ g$^{-1}$ for IMP and DS sample, respectively. Both samples have lower BET area compared to pure SBA-15 silica support, which is typically around 600-900 m$^2$ g$^{-1}$ [25,27]. The micropore volume ($V_{MI}$) was determined using $t$-plot method, and it is negligible for all samples.

The DR UV-vis spectroscopy is very often used for characterization of local

coordination of vanadium oxide species on vanadium silica samples. Figure 6 shows DR UV-vis spectra of dehydrated and fully oxidized samples diluted with pure silica [28]. The absorption below 3.2 eV, which corresponds to the presence of the non-active vanadium bulk $V_2O_5$ oxide with octahedral coordination ($O_h$), is very weak for DS sample compared to IMP sample. The absorption bands in the region of 3.2-6.3 eV belong to tetrahedrally coordinated $VO_x$ species ($T_d$) [25,28]. These units, especially the isolated $VO_4$, play the role of the most active catalytic sites in the ODH of *n*-butane [29,30]. Population of individual complexes was evaluated by means of determination of energy of absorption edge ($\varepsilon_0$). The value of energy of absorption edge was determined by using $[FR(_\infty).h]^2$ vs $h\nu$ plot [31,32]. The values of $\varepsilon_0$ for ortho-vanadate $Na_3VO_4$ (3.83 eV), meta-vanadate $NaVO_3$ (3.16 eV) and bulk $V_2O_5$ (2.26 eV) as standard compounds containing only isolated monomeric tetrahedral units, linearly polymerized tetrahedral units and octahedrally coordinated oligomeric units, respectively, were used for the calculation of vanadium complexes population [33]. The absorption edge of IMP and DS sample is 3.5 eV and 3.7 eV, respectively (see Table II). Relative amount of monomeric units was calculated based on the linear dependence of the $\varepsilon_0$ value of physical mixture of ortho- and meta-vanadate on the composition of this mix-e

Table II   Parameters of diffuse reflectance UV-vis spectra and $H_2$-TPR of vanadium mesoporous materials

| Sample name | $\varepsilon_0$[a] eV | $T_{1,max}$ °C[b] | $T_{2,max}$ °C[b] | $\Delta e$[c] |
|---|---|---|---|---|
| IMP | 3.5 | 572 | - | 1.7 |
| DS | 3.7 | 620.9 | 757 | 1.9 |

[a]Energy of absorption edge calculated by Tauc's method
[b]Position of maxima of $H_2$-TPR profile
[c]Average oxidation state change during $H_2$-TPR up to 900 °C

ture as introduced by Tian *et al.* [34]. The linear function can be expressed as follows: $X = -4.623 + 1.468\,\varepsilon_0$, where $X$ is the relative amount of monomeric species, $\varepsilon_0$ is the value of absorption edge determined from experimental spectrum of the sample. Based on this relationship, relative population of monomeric units in DS sample is 80.8 %, while for IMP sample only 51.5 %. Therefore, it can be concluded that DS sample exhibits better dispersion of vanadium species on the silica surface.

For the check of accessibility of active vanadium species we carried out $H_2$-TPR experiment. The change in the oxidation state during the reduction process, which corresponds to overall hydrogen consumption during $H_2$-TPR experiment, was 1.7 and 1.9 of electrons per vanadium atom for IMP and DS samples, respectively (Table II). This value is very close to 2 which correspond to quanti-
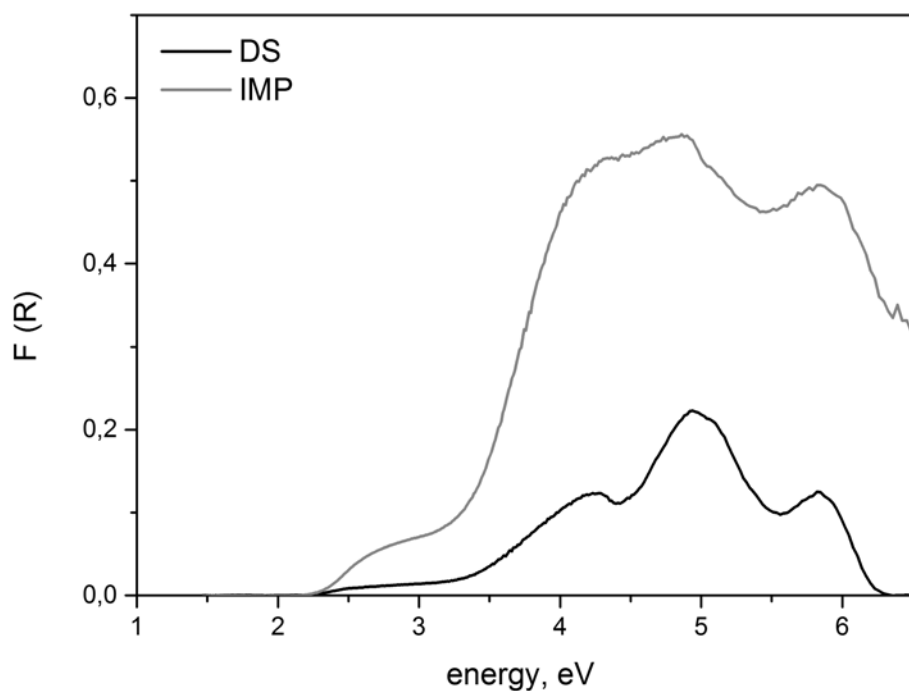
Fig. 6  DR UV-vis reflectance spectra of diluted and dehydrated samples (dilution ratio 1:100)
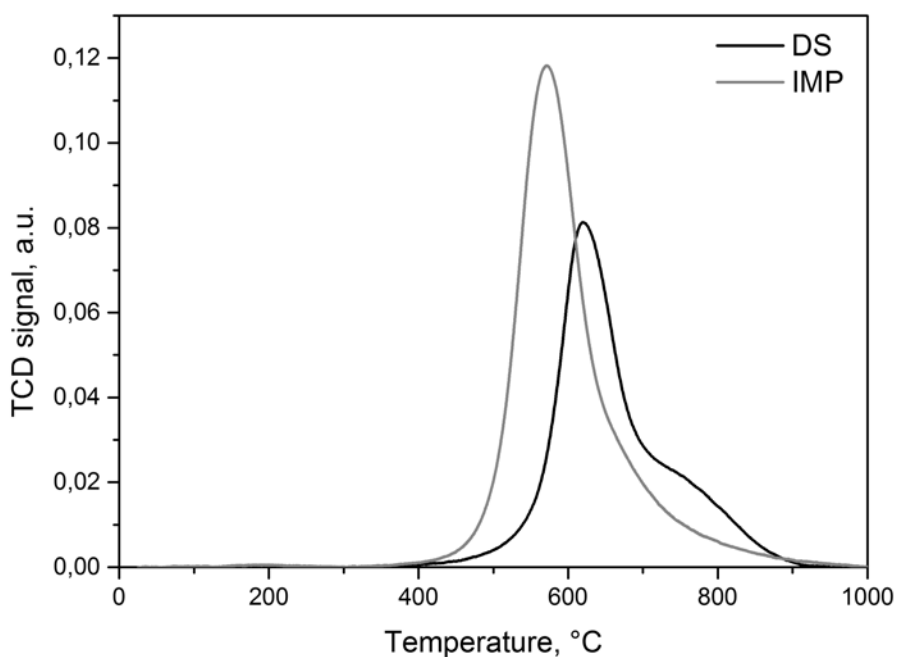


Fig. 7  $H_2$-TPR patterns of samples prepared by impregnation method (IMP), direct synthesis (DS)

tative reduction of $V^{+V}$-$V^{+III}$. These results indicate that the most of vanadium $VO_x$ species are accessible for both samples. The shapes of reduction peaks in $H_2$-TPR pattern of both samples significantly differs. The TPR pattern of impregnated sample shows only one $H_2$-TPR peak with maximum at 572 °C, while the pattern of direct synthesis sample consists of reduction peak at 621 °C with broader

shoulder at the temperature range of 720-860 °C (see Fig. 7). This shoulder can be (probably) associated with the energy demanding reduction of vanadium species, which are more buried in the wall of support; therefore, the reduction process is slower. This kind of $VO_x$ species is only typical of the samples prepared by direct synthesis method. Higher temperature of low-temperature peak in the TPR pattern of DS sample could be another evidence of a higher population of monomeric species, which can exhibit less reducible behaviour compared to polymeric species on the silica surface.

Nature of vanadium species and their reducibility were investigated also by FT-IR spectroscopy of adsorbed NO molecules, which interact with vanadium species in lower oxidation states. In our previous study[35], we performed detailed description of the main spectra of the sample with 9 wt.% of V before and after reduction by hydrogen at 450 °C for 3 h. In this study, we did not observe principal differences between the main spectra of both samples; therefore, we are focused on the spectra of adsorbed NO at RT on reduced samples. NO is a suitable probe molecule due to better distinguishing of $V^{4+}$ and $V^{3+}$ complexes compared with CO. Adsorption of NO on reduced samples leads to the appearance of a series of bands with maxima at 1906, 1833, 1761, 1728, 1696 and 1625 $cm^{-1}$ (Figs 8 and 9). It is well known that both $V^{4+}$ and $V^{3+}$ cations form dinitrosyl species characterized by asymmetric and symmetric vibrations. The $V^{4+}(NO)_2$ complexes display $v_s$ at 1920-1880 $cm^{-1}$ and $v_{as}$ at 1785-1753 $cm^{-1}$ [36-38]. The $v_s$ modes for $V^{3+}(NO)_2$ are observed at 1835-1822 $cm^{-1}$ and the respective asymmetric modes, at 1705-1685 $cm^{-1}$. The band at 1724 $cm^{-1}$ was assigned to mononitrosyls of $V^{3+}$ [35]. At low coverage intensity of the bands characterized $V^{4+}(NO)_2$ complexes on the sample with 9 wt. % of V split into two components with the maxima at 1774 and 1749 $cm^{-1}$, while on the sample with 6.6 wt. % of V such well-defined splitting was not observed. If we look more carefully on the bands characterized as $v_s$ and $v_{as}$ of $V^{4+}(NO)_2$ complexes on the sample (6.5 wt.% of V), we will see that the bands consist of two components with the maxima at 1906, 1883 $cm^{-1}$ for $v_s$ and 1761, 1753 $cm^{-1}$ for $v_{as}$. The bands at 1907 $cm^{-1}$ also consist of two components, but the splitting is very low ($\sim 2$ $cm^{-1}$). This splitting of the band was observed by Venkov *et al*. [39] on V-SBA-15 and Ivanova *et al*. [36] on VSiBEA. The authors suggested the existence of two types of $V^{4+}(NO)_2$ dinitrosyls.

Evacuation at ambient temperature (Fig. 8 spectra a-o and Fig. 9 a-h) provokes decreasing in intensity of $V^{4+}(NO)_2$ and $V^{3+}(NO)_2$ complexes. The $V^{4+}(NO)_2$ complexes on the sample obtained by direct synthesis are more stable upon evacuation compared to the same complexes on the sample with 9 wt. %. On the other hand, the stability of $V^{3+}$ mononitrosyls on the sample with 9 wt. % is higher compared with the sample obtained by direct synthesis. The ratio between the intensity of the bands describing symmetric and asymmetric stretching modes of dinitrosyls depends on the angle between the molecules. This ratio for $V^{3+}(NO)_2$ on the sample with 9 wt. % of V is higher compared with the same ratio for the
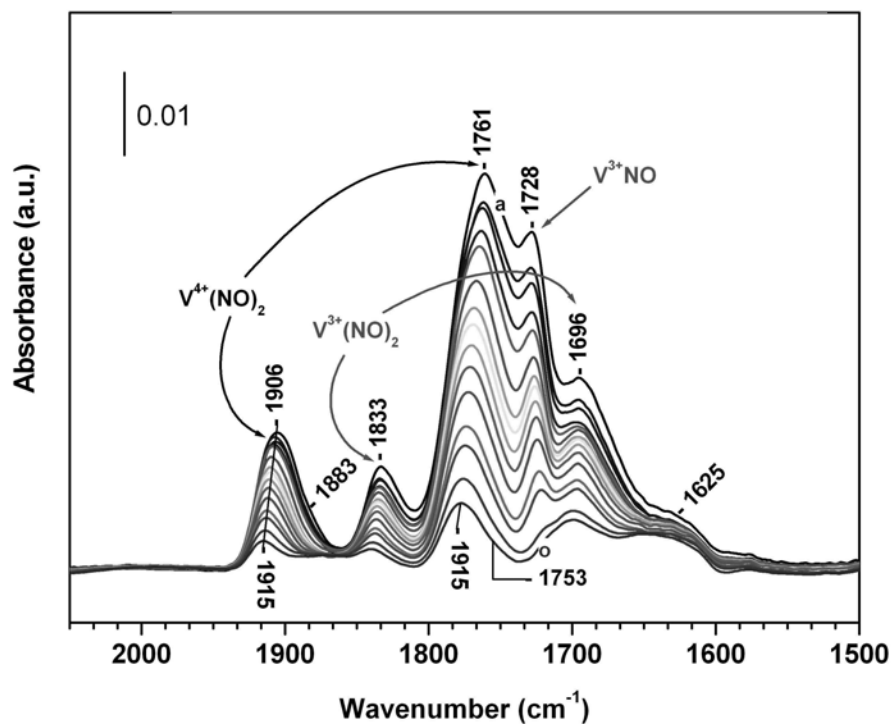
Fig. 8  FTIR spectra of NO (10 Pa equilibrium pressure) adsorbed at RT on direct synthesis sample containing 6.6 wt. % of V. Evolution of the spectra during evacuation at room temperature (a-o). The spectra are background corrected
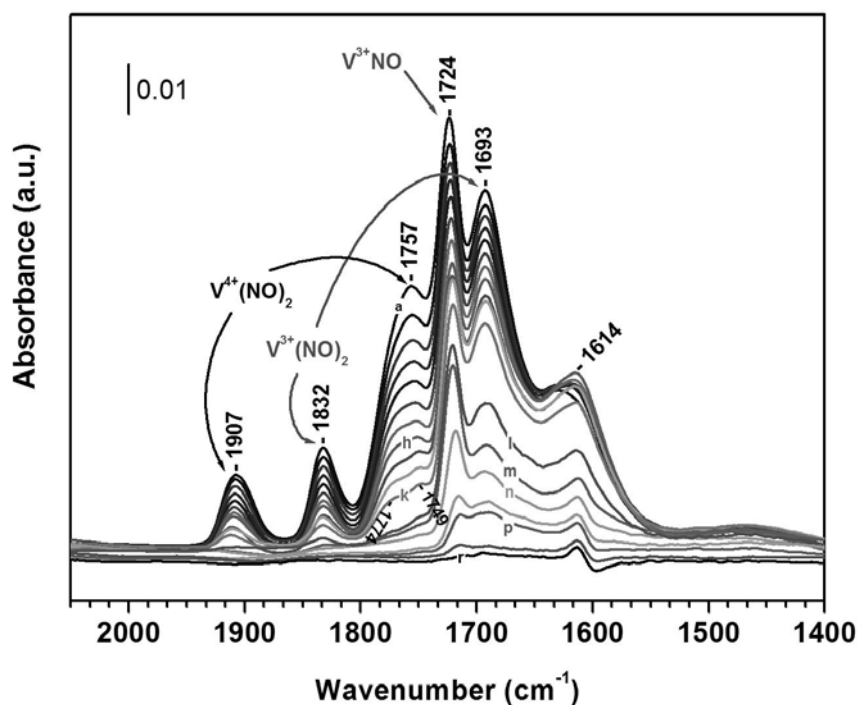


Fig. 9  FTIR spectra of NO (80 Pa equilibrium pressure) adsorbed at RT on impregnated sample containing 9 wt. % of V. Evolution of spectra during evacuation at room temperature (a-h), at 50 °C for 3, 5 and 10 min (i-k), at 80 °C 3 min (l), at 100 °C 3 min (m), at 110 °C 5, 10 and 10 min (n-p) and at 150 °C 5 and 10 min (q-r). Spectra are background corrected

sample obtained by direct synthesis because of a larger angle between the NO molecules. The intensity of the bands of $V^{4+}(NO)_2$ complexes is higher compared to the intensity of the $V^{3+}(NO)_2$ complexes (Fig. 8) on the sample obtained by direct synthesis, while on the sample obtained by impregnation method we observed the opposite case (Fig. 9). This observation is in a good agreement with TPR results, which showed that the reduction of vanadium in the DS sample takes place at a lower rate (reduction peak is observed at higher temperature) than the reduction in IMP sample. The bands at 1621 cm$^{-1}$ and 1614 cm$^{-1}$ remain relatively stable upon evacuation at ambient temperature. These bands were assigned to nitro [39,40] or nitrato compounds [36] formed upon adsorption of NO on polymeric vanadium species. The intensity of these bands is higher for IMP sample, which can indicate higher population of polymeric clusters of vanadia in this sample. This observation is in agreement with higher intensity of the bands below 3.2 eV and lower value of edge of absorption energy for IMP sample in DR UV-vis spectra.


Catalytic Tests of Propane ODH

Oxidative dehydrogenation of propane over the investigated samples was studied at 540 °C at various contact times realized by changes in catalyst weight. Main results are presented in Table III. The main reaction products identified in the reaction mixture were propene and carbon oxides. Traces of ethene and methane were detected as cracking products. No oxygenates were observed, and the carbon balance was 93 ± 5 %. The propane conversion over empty reactor (filled only with 2 ml SiC) was lower than 0.4 % under the same conditions of feed and temperature. Therefore, we can exclude participation of gas phase reaction or reaction over SiC under these reaction conditions. It is well-known that the selectivity is necessary to be compared at the same degree of conversion for parallel-consecutive reaction such as the C$_3$-ODH reaction. Therefore, the catalytic behaviour of vanadosilicate catalysts with different vanadium loading and different methods of preparation was compared under iso-conversion conditions at propane conversion degree of 13 %. In addition, catalytic performance of the samples only slightly depended on time-on-stream (decline of propane conversion and propene selectivity was 1 and 2 %, respectively, within 4 h in the stream). Therefore, the data after 2 h in the stream were taken for catalysts comparison. Despite the fact that the samples differ in the vanadium content and relative population of vanadium complexes, both samples exhibit the identical catalytic activity expressed by turn over frequencies (TOF). It should be noted that the TOF is the average number of catalytic cycles at one average vanadium atom per time unit; the value usually strongly depends on the population of individual vanadium complexes. Therefore, it means that both monomeric and oligomeric $T_d$ species presented in the samples are active sites for C$_3$-ODH reaction with the same (or

very similar) activity. This agrees with previously published observation for $VO_x$-HMS catalysts [41]. Although both samples exhibit the same *TOF*, the productivity of DS sample is higher due to much higher selectivity to propene: about 23 % higher value of this selectivity than with the impregnated sample (see Table II). Changes in isoconversional selectivity towards propene are reflected in changes in selectivity towards CO, while selectivity toward $CO_2$ is constant (about 14 %). It is very interesting that $CO_2$ selectivity is quite constant with a wide range of vanadium based mesoporous silica catalysts as was mentioned earlier [42].

Table III  Results of catalytic tests in oxidative dehydrogenation of propane at 540 °C and iso-conversion of propane 13 % ($C_3H_8/O_2/He$ = 5/2.5/92.5 vol. %, total flow rate of 100 $cm^3$ $min^{-1}$)

| Catalytic system | $T$ °C | $w_V$ wt. % | Conversion, % | | Selectivity, % | | | |
|---|---|---|---|---|---|---|---|---|
| | | | $C_3H_8$ | $O_2$ | $C_3H_6$ | $C_1$-$C_2$[a] | CO | $CO_2$ |
| IMP | 540 | 9 | 13 | 62 | 48 | 0 | 38 | 14 |
| DS | 540 | 6.5 | 13 | 60 | 71 | 0 | 16 | 13 |

| Catalytic system | *TOF* $h^{-1}$ | Productivity[b] $C_3H_6$ |
|---|---|---|
| IMP | 13 | 0.38 |
| DS | 13 | 0.48 |

[a]$C_1$-$C_2$ – sum of $C_1$-$C_2$ hydrocarbons
[b]Productivity – $kg_{prod}$ $kg_{cat}^{-1}$ $h^{-1}$

## Conclusion

Two vanadium-containing mesoporous silica catalysts were synthesized by different techniques (including direct synthesis from hydrogel containing vanadium precursor and wet impregnation of SBA-15 mesoporous silica by vanadyl acetylacetonate) and their physico-chemical and catalytic properties were studied and compared. Based on the results reported heretofore, we can conclude that direct synthesis of vanadosilicate led to catalysts with non-uniform mesoporosity, but exhibiting better spreading of vanadium on the surface resulting in species with lower degree of polymerization compared to impregnated catalyst. Vanadium species in the sample prepared by direct synthesis exhibit lower reducibility reflected in a higher temperature of reduction in $H_2$-TPR and higher population of $V^{4+}$ oxidation state in the IR spectra of adsorbed NO on the samples reduced in the static hydrogen atmosphere at 450 °C. It is reflected in higher iso-conversional selectivity of directly synthesized catalyst towards propene.

## Acknowledgement

## References

[1]    Guo Z., Zhou C.M., Hu S.Q., Chen Y.T., Jia X.L., Lau R.M., Yang Y.H.: Appl. Catal. A-Gen. **419**, 194 (2012).

[2]    Liu Y.-M., Cao Y., Zhu K.K., Yan S.R., Dai W.L.: Chem. Commun., 2832 (2002).

[3]    Jones J., Ross J.R.H.: Catal. Today **35**, 97 (1997).

[4]    Krishnamoorthy S., Baker J.P., Amiridis M.D.: Catal. Today **40**, 39 (1998).

[5]    Delaigle R., Debecker D.P., Bertinchamps F., Gaigneaux E.M.: Top. Catal. **52**, 501 (2009).

[6]    Bertinchamps F., Treinen M., Eloy P., Dos Santos A.M., Mestdagh M.M., Gaigneaux E.M.: Appl. Catal. B-Environ. **70**, 360 (2007).

[7]    Cavani F., Ballarini N., Cericola A.: Catal. Today **127**, 113 (2007).

[8]    Ying F., Li J.H., Huang C.J., Weng W.Z., Wan H.L.: Catal. Lett. **115**, 137 (2007).

[9]    Piumetti M., Bonelli B., Armandi M., Gaberova L., Casale S., Massiani P., Garrone E.: Microporous Mesoporous Mat. **133**, 36 (2010).

[10]  Piumetti M., Bonelli B., Massiani P., Millot Y., Dzwigaj S., Gaberova L., Armandi M., Garrone E.: Microporous Mesoporous Mat. **142**, 45 (2011).

[11]  Gao F., Zhang Y.H., Wan H.Q., Kong Y., Wu X.C., Dong L., Li B.Q., Chen Y.: Microporous Mesoporous Mat. **110**, 508 (2008).

[12]  Parmaliana A., Sokolovskii V., Arena F., Frusteri F., Miceli D.: Catal. Lett. **40**, 105 (1996).

[13]  Corma A., Nieto J.M.L., Paredes N.: J. Catal. **144**, 425 (1993).

[14]  Gao X.T., Ruiz P., Xin Q., Guo X.X., Delmon B.: J. Catal. **148**, 56 (1994).

[15]  Scharf U., Schramlmarth M., Wokaun A., Baiker A.: J. Chem. Soc. Faraday Trans. **87**, 3299 (1991).

[16]  Sato S., Toita M., Sodesawa T., Nozaki F.: Appl. Catal. **62**, 73 (1990).

[17]  Zukal A., Šiklová H., Čejka J.: Langmuir **24**, 9837 (2008).

[18]  Kubelka P., Munk F.: Z.Tech. Phys. **12**, 593 (1931).

[19]  Sachtler W.M.H., Boer N.H.D.: Proc. 3rd Int. Congr. Catalysis (1964).

[20]  Galarneau A., Cambon N., Di Renzo F., Ryoo R., Choi M., Fajula F.: New J. Chem. **27**, 73 (2003).

[21] Zhao D.Y., Feng J.L., Huo Q.S., Melosh N., Fredrickson G.H., Chmelka B.F., Stucky G.D.: Science **279**, 548 (1998).

[22] Zhao D.Y., Sun J.Y., Li Q.Z., Stucky G.D.: Chem. Mat. **12**, 275 (2000).

[23] Meynen V., Cool P., Vansant E.F.: Microporous Mesoporous Mat. **125**, 170 (2009).

[24] Vunain E., Malgas-Enus R., Jalama K., Meijboom R.: J. Sol-Gel Sci. Technol. **68**, 270 (2013).

[25] Bulánek R., Kalužová A., Setnička M., Zukal A., Čičmanec P., Mayerová J.: Catal. Today **179**, 149 (2012).

[26] Weckhuysen B.M., Keller D.E.: Catal. Today **78**, 25 (2003).

[27] Liu W., Lai S.Y., Dai H.X., Wang S.J., Sun H.Z., Au C.T.: Catal. Lett. **113**, 147 (2007).

[28] Bulánek R., Čapek L., Setnička M., Čičmanec P.: J. Phys. Chem. C **115**, 12430 (2011).

[29] Setnička M., Bulánek R., Čapek L., Čičmanec P.: J. Mol. Catal. A-Chem. **344**, 1 (2011).

[30] Setnička M., Čičmanec P., Bulánek R., Zukal A., Pastva J.: Catal. Lett. **144**, 50 (2014).

[31] Tauc J.: *Amorphous and Liquid Semiconductors*, Plenum Press, London, 1974.

[32] Davis E.A., Mott N.F.: Philos. Mag. **22**, 903 (1970).

[33] Gao X.T., Wachs I.E.: J. Phys. Chem. B **104**, 1261 (2000).

[34] Tian H.J., Ross E.I., Wachs I.E.: J. Phys. Chem. B **110**, 9593 (2006).

[35] Bulánek R., Drenchev N., Čičmanec P., Setnička M.: Adsorpt.-J. Int. Adsorpt. Soc. **19**, 339 (2013).

[36] Ivanova E., Hadjiivanov K., Dzwigaj S., Che M.: Microporous Mesoporous Mat. **89**, 69 (2006).

[37] Hadjiivanov K.I., Vayssilov G.N.: Adv. Catal. **47**, 307 (2002).

[38] Hadjiivanov K.I.: Catal. Rev.-Sci. Eng. **42**, 71 (2000).

[39] Venkov T.V., Hess C., Jentoft F.C.: Langmuir **23**, 1768 (2007).

[40] Hess C.: Chem. Phys. Chem. **10**, 319 (2009).

[41] Bulánek R., Čičmanec P., Sheng-Yang H., Knotek P., Čapek L., Setnička M.: Appl. Catal. A-Gen. **415**, 29 (2012).

[42] Yang H., Liu Z., Gao H., Xie Z.: Catal. Today **216**, 90 (2013).